SSC-N-651
June 89

BEAM-BEAM TUNE MODULATION, THE DRIVEN GRAVITY PENDULUM, AND JOSEPHSON JUNCTIONS

Tong Chen* and Stephen Peggs

SSC Central Design Group†
c/o Lawrence Berkeley Laboratory
One Cyclotron Road
Berkeley, CA 94720

INTRODUCTION

Most contemporary electron and proton storage rings are limited in their performance by the beam-beam effect. Consider a test particle passing through a counter-rotating bunch of particles at a nominal collision point of a storage ring—without a hard collision. The test particle experiences macroscopic electric and magnetic fields which give its trajectory a nonlinear kick. For example, a proton displaced horizontally by X, passing through a round Gaussian bunch of size σ, receives an angular kick

$$\Delta X' = -\frac{4\pi\xi}{\beta}\frac{2\sigma^2}{X}\left[1-\exp\left(\frac{-X^2}{2\sigma^2}\right)\right] \qquad [1]$$

where ξ, the "tune shift parameter," is proportional to the transverse charge density in the bunch. The strength of the kick drops off like 1/X at large displacements, unlike the polynomial behavior of magnetic kicks, since the nonlinear field source is localized at the center of the beam pipe. Small amplitude trajectories receive kicks which are linear in displacement, as in a quadrupole, and are shifted in tune by ξ—hence the name, tune shift parameter. At large amplitudes the tune shift approaches zero, and the situation is usually stable, again in contrast to the magnetic case. Beam-beam resonances are strongest at intermediate amplitudes of a few sigma.

Accelerator physics is in good company when it considers the problem of single particle stability in response to nonlinear forces such as the beam-beam interaction. For example, the question of the stability of the solar system is perhaps the best known and longest standing problem in nonlinear dynamics. Here is a system with an age of order 10^{10} periods (years), which, despite the best efforts of generations of mathematicians, has not been proven to be stable. Rigorous mathematical results are hard to come by in even the simplest nontrivial systems, like the three body problem. More valuable than rigorous results, however, are the analytic languages and tools which classical dynamicists have established in their studies of differential systems—systems which are naturally described by differential equations.

The relatively recent advent of powerful computers caused an explosion in the interest paid to nonlinear problems. Computers, by their cyclical iterative nature, tend to make problems look like difference equations. On the other hand, analytic tools tend to make problems look like differential equations, since they are usually much easier to solve than difference equations, requiring only pencil and paper. Which representation is truly appropriate depends on the nature of the system involved. For example, it is natural to represent the solar system as a differential system, since gravity acts smoothly and continuously, while the beam-beam interaction is naturally a difference system, since the nonlinear perturbations are well-represented by brief impulses, separated by lengthy sections of linear motion.

Despite all the powerful analytic and numerical tools available, it is still impossible to prove the long-time scale stability of trajectories. At this point a physicist resorts to the traditional defense that pragmatism is more important than rigor. The solar system appears to be comfortably stable for 10^{10} periods. Proton storage rings such as the SPS and the Tevatron, with circulation frequency of about 40 kHz and storage times of about one day, are conservative nonlinear systems which are usefully stable for about 4.10^9 periods. In contrast, the SSC, with a revolution frequency of about 3.5 kHz (the first man-made audio frequency accelerator), needs stability for only about 3.10^8 turns in order to provide collisions for one day. While the time span of the problem has shortened, the time span of the available tools has lengthened—it is no longer uncommon to follow computer simulations of accelerator models for 10^6 turns. Although simulations still fall short of the SSC time scale by about two orders of magnitude, it is reasonable to accept their predictions about the behavior of the SSC, if the simulations agree with the real behavior of existing accelerators operating under relevant nonlinear conditions.

The maximum operational tune shift parameter is of order 0.02 per collision in electron rings, and of order 0.004 per collision in proton rings. This order of magnitude difference is largely due to the difference in transverse beam shape (electron beams are flat, proton beams are round, both are bi-Gaussian) and to the fact that electrons produce a lot of synchrotron radiation, leading indirectly to a stabilizing damping of the transverse motion. The SSC will be the first proton storage ring in which synchrotron radiation is significant, with a damping time of about half a day. Electron ring damping times are typically measured in milliseconds. Somewhat different theoretical models are used to successfully explain the beam-beam limits in the two kinds of ring [1–5]. Good quantitative agreement between theory, simulation, and observation is obtained, in the proton case, only when tune modulation effects are taken into account [6–10].

This paper concentrates on the problem of describing the response of an accelerator resonance—beam-beam or otherwise—to an external tune modulation perturbation. In particular, the qualitatively different responses in four separate regions of configuration space are quantitatively explained by merging piecemeal theories which are individually valid in only limited circumstances. At first sight this concentration appears to be on a beam-beam effect of only limited scope—of limited relevance to electron storage rings, for example. In fact, it is a subject of broad general interest across nonlinear dynamics, describing, amongst other systems, the behavior of the Josephson junction as used in defining the standard Volt [11–14]. The equations of motion of both of these systems are analogous to these of a gravity pendulum, driven by a sinusoidal torque.

THE DRIVEN DIFFERENTIAL PENDULUM

The most compact way to describe the motion of a differential pendulum of mass M, length L, acting under the acceleration due to gravity g, is by means of the Hamiltonian,

$$H = \frac{1}{2}\frac{p^2}{ML^2} - MLg\cos(\theta) \equiv \frac{1}{2}Up^2 - V\cos(\theta) \qquad [2]$$

---

* Visitor from the Institute of HEP, Academia Sinica, Peking

† Operated by the Universities Research Association, Inc., for the U. S. Department of Energy.

where θ is the angle the pendulum makes with the vertical, and p is the angular momentum,

$$p = ML^2 \frac{d\theta}{dt} \qquad [3]$$

Equation [2] is, by definition, shorthand for the equations of motion

$$\frac{d\theta}{dt} = \frac{\partial H}{\partial p}$$
$$\frac{dp}{dt} = -\frac{\partial H}{\partial \theta} \; . \qquad [4]$$

Trajectories of the pendulum system follow contours of the Hamiltonian function, because H is explicitly conserved, since

$$\frac{dH}{dt} = \frac{\partial H}{\partial p}\frac{dp}{dt} + \frac{\partial H}{\partial \theta}\frac{d\theta}{dt} = 0 \qquad [5]$$

by substitution of the equations of motion [4]. The rate of progress along a contour depends only on the local slope of the Hamiltonian function. A particular pendulum is conveniently represented for many purposes by a single number, its free oscillation frequency in the limit of small oscillations. This quantity is called Q_I here, in a "tune" notation which is ready for analogy with beam-beam resonances. Its value is

$$Q_I = \frac{1}{2\pi}(UV)^{1/2} = \frac{1}{2\pi}\left(\frac{g}{L}\right)^{1/2} . \qquad [6]$$

When the pendulum is driven by an external torque of amplitude T which is varying sinusoidally in time, it is no longer so easy to describe the motion by means of a Hamiltonian—although it is still possible in some cases, as will be shown below. The equation of motion of the pendulum is now

$$\frac{d^2\theta}{dt^2} + (2\pi Q_I)^2 \sin(\theta) = T\cos(2\pi Q_M t) \; . \qquad [7]$$

So long as the motion of the pendulum is periodic, and not chaotic, it is convenient to expand θ as a double Fourier series expansion, in the drive tune Q_M and in a free oscillation tune, Q_{free}, which is in the range 0 to Q_I, depending on the amplitude of the free oscillations.

It is conceptually natural to consider the free oscillations as trivially superimposed on the driven motion, which contains most of the interesting physics of the situation. This perspective is also appropriate in experimental investigations of the system, such as in the E778 nonlinear dynamics experiment [15-20], and in the mechanical modeling of Josephson junctions [11-13]. Ignoring the free oscillations, then, there is a family of *possible* periodic solutions labeled by the integer k,

$$\theta = k\,2\pi(Q_M t) + \sum_{n=1}^{\infty} c_n \cos(n\,2\pi Q_M t) \qquad [8]$$

where the coefficients c_n are functions of the configuration variables, T, Q_M, and Q_I. The pendulum rotates exactly k complete turns in one modulation period.

In the accelerator representation of this system, where the tune is modulated, the family of solutions corresponds to a family of synchro-betatron sidebands, as will be shown below. That is, particles in a tune-modulated accelerator are free to oscillate about any stable member of a family of sideband resonances, each of which has a tune Q_k which is offset from a fundamental resonance by an amount proportional to k,

$$Q_k = \frac{m}{n} + k\frac{Q_M}{n} \; . \qquad [9]$$

Since the persistent signal due to protons trapped in a resonance island is an experimental observable, then it is possible to observe a signal at any of the Q_k tunes, if the signal is strong enough.

For a particular sideband to be observed in practice, it must not only be stable, but must also be of significant size. Persistent synchro-betatron signals (with non-zero k) have already been seen in the analysis of E778 data taken in 1988, although not so cleanly as to justify publication. It is expected that the more sensitive electronics which will be used in the 1989 run will compensate for the limited reach in the E778 configuration plane, so that many such signals will be available for quantitative analysis.

Equation [7] also describes a Josephson junction, when it is driven by a radio frequency current source at a frequency Q_M. In this representation the angle θ is the quantum phase difference across the junction. The voltage across the junction is proportional to the instantaneous rate of change of θ, with a multiplicative constant which depends only on the fundamental quantities e and h, the electronic charge and Planck's constant. After differentiating the solution [8], then, the voltage across a driven Josephson junction is

$$V_k = k\frac{h}{e}\frac{Q_M}{4\pi} + \text{alternating terms} \qquad [10]$$

where the alternating terms can be neglected. The precision with which the family of these voltages is known can be used to define the standard Volt. Typically, frequencies of order 10 GHz, and k values as large as 100, are used to produce voltages of order 100 μV per junction [14]. It is possible to lithograph as many as 10^4 of these junctions in series on a single chip, to make well-known voltages of order 1 Volt. It should be noted in passing that the voltages are stable despite the presence of significant damping in the Josephson system, which is not included in equation [7].

The simple and fundamental theme of this paper can be defined by asking two questions in a context-free manner: Is the k-th solution of [8] stable for given Q_I, Q_M, and T? If it is stable, does it have a significant size or strength? It is nonetheless convenient and appropriate to answer the questions in the specific context of accelerator resonances. Finally, note that although there appears to be three configuration variables, only two of them are independent, since (for example) Q_I can be normalized to one by redefining the unit of time. Such a normalization would be confusing to the intuition, since the natural unit of time in the accelerator system is emphatically a single turn. Therefore, in what follows, Q_I is almost always simply assumed to be constant, leaving T and Q_M, (or their analogs) to be the configuration variables.

ACCELERATOR EQUATIONS OF MOTION

The simplest way to describe linear motion in an accelerator is in terms of "normalized" phase space coordinates, (x,x'), which are related to the "physical" coordinates by the transformation

$$\begin{pmatrix} x \\ x' \end{pmatrix} = \begin{pmatrix} \frac{1}{\sqrt{\beta(s)}} & 0 \\ \frac{\alpha(s)}{\sqrt{\beta(s)}} & \sqrt{\beta(s)} \end{pmatrix} \begin{pmatrix} X \\ X' \end{pmatrix}, \quad \alpha = -\frac{1}{2}\beta' \; . \qquad [11]$$

Here $\beta(s)$ is the "betatron function" which characterizes the linear optical focusing properties as a function of azimuthal position. In this frame linear motion is generally described by

$$\begin{pmatrix} x(s) \\ x'(s) \end{pmatrix} = a_0 \begin{pmatrix} \sin(\phi(s) - \phi_0) \\ \cos(\phi(s) - \phi_0) \end{pmatrix} \; . \qquad [12]$$

That is, motion from one azimuth to another is described by a simple smooth rotation around a circle of constant radius, with a rate of advance given by

$$\frac{d\phi}{ds} = \frac{1}{\beta} \quad . \qquad [13]$$

So, in a normalized phase space description of linear motion the trajectory fibers form a bundle which is circularly symmetric, where all the fibers turn around the center of the bundle at the same rate.

In order to describe nonlinear motion, it is convenient to introduce "action-angle" coordinates, J and ϕ, where

$$\begin{pmatrix} x \\ x' \end{pmatrix} = \begin{pmatrix} (2J)^{1/2}\sin(\phi) \\ (2J)^{1/2}\cos(\phi) \end{pmatrix} . \qquad [14]$$

That is, the action J behaves very much like the betatron amplitude, while ϕ is explicitly the betatron phase of the trajectory under study. It is usually possible to describe the motion from turn t to t + 1 at a fixed azimuthal location in terms of a "discrete" Hamiltonian, H_1.

$$\begin{pmatrix} J \\ \phi \end{pmatrix}_{t+1} \approx \begin{pmatrix} J \\ \phi \end{pmatrix}_t + \begin{pmatrix} -\dfrac{\partial H_1}{\partial \phi} \\ \dfrac{\partial H_1}{\partial J} \end{pmatrix}_t . \qquad [15]$$

The approximation sign is necessary here not only because the function $H_1(J,\phi)$ is typically only correct to first order in the perturbation strength (for example the beam-beam tune shift parameter) but also because the motion described is not area-preserving, or symplectic. This is because of the discrete nature of the motion. If the difference equation [15] were, instead, a differential equation, as in [4], then the motion would at least be proper, even if incorrect due to the approximate nature of the Hamiltonian.

Five Islands—the Single Resonance Hamiltonian, H_5

When the amplitude of a trajectory is small—as $J \to 0$ — the single turn phase advance given by [15] tends towards a constant, $2\pi Q_0$, where Q_0 is the "base tune" of the accelerator. Since Q_0 is typically not close to an integer, there is usually a large change of phase (modulo 2π) in one turn. However, if the fractional part of the base tune is close to a rational fraction, 2/5 for a convenient example, then after 5 turns around the ring the net change in phase can be rather small, and resonant motion is important.

If the strongest nonlinear elements are sextupoles, then it can be shown [20] that when the motion in [15] is iterated 5 times—"when H_1 is averaged over 5 turns"—the leading components of the "single-resonance Hamiltonian" have the general form

$$H_5 = 2\pi(Q_0 - \tfrac{2}{5})J + V_4 J^2 - V_5 J^{5/2}\cos(5\phi + \phi_5) \qquad [16]$$

which is just shorthand for the five-turn difference equation of motion

$$\begin{pmatrix} J \\ \phi \end{pmatrix}_{t+5} \approx \begin{pmatrix} J \\ \phi \end{pmatrix}_t + 5\begin{pmatrix} -\dfrac{\partial H_5}{\partial \phi} \\ \dfrac{\partial H_5}{\partial J} \end{pmatrix}_t \qquad [17]$$

by analogy with equation [15].

The meaning of the three terms in H_5 becomes clear when the partial differentiations in [17] are performed. For example, the first term corresponds to a five-turn phase advance of $5 \cdot 2\pi\{Q_0 - (2/5)\}$, independent of the action. Subtraction of 2/5 from Q_0 is justified by noting that it leads to an inconsequential subtraction of 4π from the five-turn phase advance. The subtraction is motivated by making the coefficient of J a small number. Next, differentiation of $V_4 J^2$ with respect to J leads to a five-turn phase advance of $10 V_4 J$, linearly proportional to the action.

$$Q(J) = Q_0 + \frac{V_4}{\pi} J = Q_0 + \frac{V_4}{2\pi} a^2 \qquad [18]$$

That is, there is an octupolar tune shift with action or amplitude.

For comparison with the contours of equation [16], Figure 1 shows the simulated motion of protons stored in the Tevatron, when a Q = 2/5 resonance is driven by 16 special sextupoles under the experimental conditions of E778 [17]. The tune drops from about 19.42 at the center (small oscillations), through 19 + 2/5, where five islands can be seen, down to 19 + 1/3, at the dynamic aperture of the Tevatron in this particular configuration. Note that the five islands are distorted by the triangular structure, which is absent from the approximate Hamiltonian description of equation [16].

The action J_I at which $Q(J_I) = 2/5$ identifies where the resonance is found. Before examining the behavior of the term in V_5, it is convenient to make a coordinate transformation and rewrite H_5 as an expansion around J_I,

$$H_5 = \frac{1}{2} U I^2 - V\cos(5\phi) \qquad [19]$$

where

$$I = J - J_I, \; U = 2V_4, \; V = V_5 J_I^{5/2} \qquad [20]$$

and the value of ϕ_5 has been conveniently chosen. This resembles the pendulum Hamiltonian [2], and has the same form for beam-beam resonances (except that odd beam-beam resonances are suppressed).

Substitution of this Hamiltonian into the equations of motion [17] (with J replaced by I) shows that $(I,\phi) = (0,0)$ is a fixed point—a trajectory launched there is stationary. In some region close enough to I = 0, then, H_5 may be considered as representing differential equations of motion, continuous in t, which

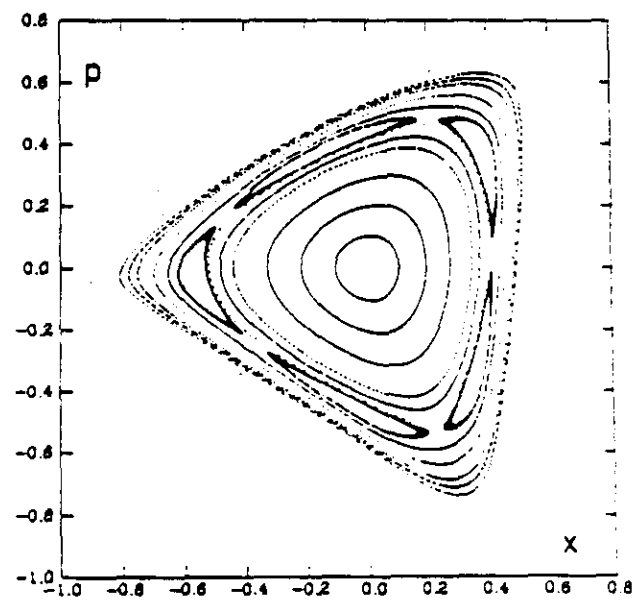

Figure 1. Surface of section plot of several trajectories, from a numerical simulation of the E778 experiment. The value of β is approximately 100 meters, so the five islands at a normalised amplitude of about $0.5\ 10^{-3}\ m^{1/2}$ have a physical amplitude of about 5.0 millimeters.

agree well with the difference motion whenever t is an integer multiple of five. In this differential perspective the "approximately equal" sign ≈ is replaced by an equality.

$$\begin{pmatrix} \frac{dI}{dt} \\ \frac{d\phi}{dt} \end{pmatrix} = \begin{pmatrix} -\frac{\partial H_5}{\partial \phi} \\ \frac{\partial H_5}{\partial I} \end{pmatrix} = \begin{pmatrix} -5V\sin(5\phi) \\ U\,I \end{pmatrix} \qquad [21]$$

Except for factors of 5, this is just the familiar case of the pendulum. For small angles, $\delta\phi << 1/5$, the solution of this equation is just

$$\begin{pmatrix} I \\ \phi \end{pmatrix} = \phi_0 \begin{pmatrix} 5\left(\frac{V}{U}\right)^{1/2} \sin(2\pi Q_I t) \\ \cos(2\pi Q_I t) \end{pmatrix} \qquad [22]$$

where it may be assumed that V and U are both positive. The free oscillation island tune is given by

$$Q_I = \frac{5}{2\pi}(U\,V)^{1/2} \qquad [23]$$

ready for direct comparison with the characteristic small angle tune of the pendulum, given by [6].

This analysis can readily be applied to the round beam-beam problem, since in that case the functions U(J) and $V_n(J)$ are analytically well known [9, 21]. Figure 2 shows the island tune Q_I which results from a single round beam-beam interaction, using equation [23] (with 5 replaced by n, the resonance order) for even order resonances up to order 12. The island tune is proportional to the tune shift parameter, with a constant of proportionality somewhat less than one. As the order of the resonance increases, the maximum value of Q_I/ξ decreases, but occurs at a normalized amplitude which is increasing. This illustrates the intermediate range nature of the beam-beam effect.

Experimental Observation of Resonances [15]

Figure 3 illustrates typical data obtained in E778, by kicking a Gaussian proton bunch into a phase space position which partially overlaps the fifth order islands shown in Figure 1. At first the signal undergoes Gaussian decoherence, appropriate to the spread of tune across the perturbed beam. However, there is also a "persistent signal," which has a very small decay rate—it is typically observed for tens of seconds, or millions of turns. This signal is due to particles which do not decohere because they are phase locked within the bounds of a resonance island. If the base tune Q_0 is adjusted to maximize the persistent signal strength, when $a_{kick} = a_I$, the persistent amplitude leads directly to the resonance island width a_W, through

$$\frac{a_{persistent}}{a_{kick}} = G\frac{a_W}{\sigma} \qquad [24]$$

where G is a geometrical factor close to unity which is calculated by numerical simulation [15, 16]. The beam size σ is assumed to be well known, although in practice it fluctuates from shot to shot. Once measurements of a_W have been made at several values of a_{kick}, the set of data pairs (Q_0, a_{kick}) may be analyzed to yield an accurate plot of tune versus amplitude.

What does theory give for the width of these islands? The amplitude width is estimated by assuming that trajectories at least as far as the separatrix follow H_5 contours. (This is explicitly wrong very close to the separatrix, which does not even exist in the difference system.) Since trajectories follow contours of H_5, and since the saddle point (unstable fixed point) is on the boundary between resonant and non-resonant motion, the height of the saddle point, $H_5(0,2\pi/10)$, is the same as the height $H_5(I_W,0)$, where I_W is the island half width. This gives

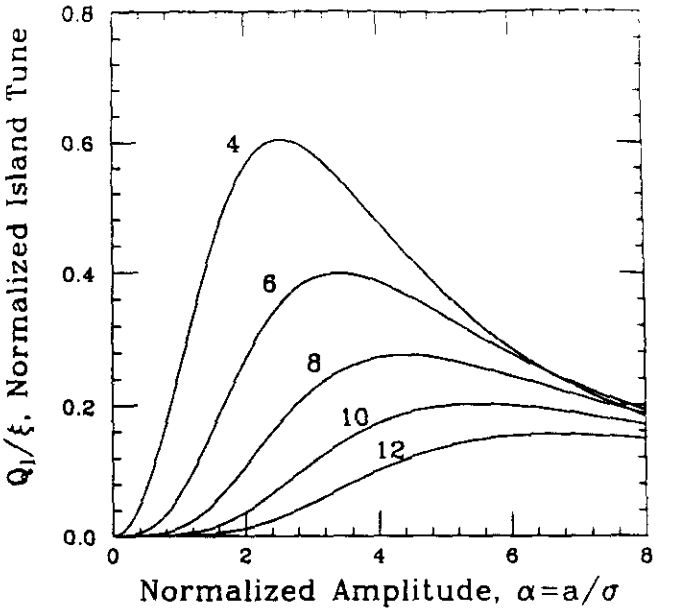

Figure 2. The ratio of island tune to tune shift parameter as a function of normalized amplitude, for a single round beam-beam interaction. The amplitude is normalized relative to the size of the opposing beam. As the order of the beam-beam resonance increases, the maximum strength of the resonance decreases, and the most potent amplitude increases. At large amplitudes the island tune tends to zero, in contrast with the case of magnetic resonances, when Q_I tends to infinity.

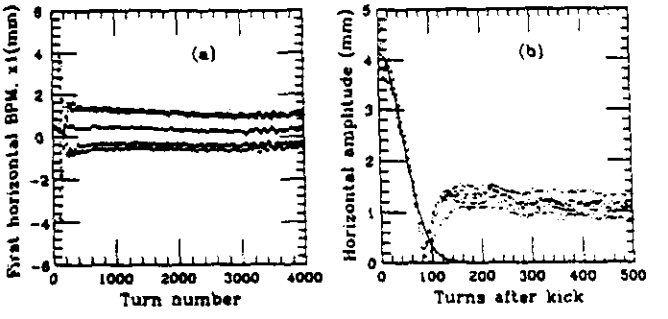

Figure 3. Typical data from the E778 experiment, showing both Gaussian decoherence and a persistent signal. a) Raw turn-by-turn data taken by one of the beam position monitors, over 4,000 turns. The signal strength initially drops very rapidly after a transverse deflection of about 4 millimeters, finally leaving five persistent signal lines with a very slow decay rate. b) The reconstructed amplitude over the first 500 turns, showing that the initial decoherence is well fitted by the solid line Gaussian. About 30% of the beam is trapped in a resonance island at an amplitude of about 4 millimeters.

$$I_W = 2\left(\frac{V}{U}\right)^{1/2} \qquad [25]$$

which is readily converted to an amplitude width, a_W.

The functions characterizing the simple Hamiltonian theory, U and V, have appeared in three expressions, for the tune shift with amplitude Q(a) [18], the island tune Q_I [23], and for the island width I_W, above. Two of these three form a complete set of experimental observables, since it is possible from any two to deduce the values of V and U at that amplitude (or

action). It is natural to choose Q(a) as the first observable, since its measurement is relatively fast and straightforward. The experience of E778 implies, however, that the second observable should be Q_I, and not I_W, because the island width measurements are relatively slow, depend on the size of the proton bunch, and, even in the best of all possible worlds, the island width varies from island to island. In contrast, the island tune Q_I is explicitly the same for all islands, has a natural intuitive definition independent of the details of the theory, (such as the presence or absence of triangular distortions) and in principle is fast to measure.

Measurements of Q_I in the 1988 run of E778 were not rapid, although great improvements are expected in 1989. The most successful of the three different measurement methods which were tried, and the only one independent of beam size, was to observe the response of a persistent signal to tune modulations of varying amplitudes and frequencies. This explains the primary relevance of tune modulation in the E778 experiment—although tune modulation phenomena are also important in their own right.

TUNE MODULATION

If a set of quadrupoles is perturbed by a small sinusoidal current, the tune of a small amplitude trajectory is modulated according to

$$Q_0 = Q_{00} + q \sin(2\pi Q_M t) \qquad [26]$$

where q and Q_M are the tune modulation amplitude and tune. Power supply ripple like this is normally carefully avoided, especially in proton colliders, where any source of noise degrades the storage lifetime of the beam. Tune modulation via the coupling of synchrotron oscillations with non-zero chromaticity is an important internal source for the beam-beam interaction, even in an otherwise perfect accelerator. Special fast quadrupoles are used during slow extraction in the Tevatron, responding to the difference between measured tune and requested tune, to ensure a steady spill rate. It is these quadrupoles which E778 uses in its investigation of resonance behavior in the (q, Q_M) parameter space. As Figure 4 shows, the (q, Q_M) plane is rich in dynamical features. The dotted line in the figure shows the region accessible to the E778 experiment, with maximum q and Q_M values of about 0.01.

Tune modulation is included in the resonance Hamiltonian near a fifth-order resonance by adding a single term to equation [19], giving

$$H_5 = 2\pi q \sin(2\pi Q_M t) I + \frac{1}{2} U I^2 - V \cos(5\phi) \ . \qquad [27]$$

This Hamiltonian is still shorthand for two differential equations, not difference equations, because of the very small net motion in five turns. Unfortunately, H_5 is now time dependent, and so is no longer conserved. The two first-order equations of motion are now

$$\begin{pmatrix} \frac{dI}{dt} \\ \frac{d\phi}{dt} \end{pmatrix} = \begin{pmatrix} -5V \sin(5\phi) \\ 2\pi q \sin(2\pi Q_M t) + UI \end{pmatrix} \qquad [28]$$

or, as a single second-order differential equation in ϕ

$$\frac{d^2\phi}{dt^2} + (2\pi Q_I)^2 \frac{\sin(5\phi)}{5} = (2\pi)^2 q Q_M \cos(2\pi Q_M t) \ . \qquad [29]$$

This is directly analogous to the motion of a rigid pendulum, of small amplitude natural tune Q_I, shown in equation [7]. (The factors of 5 can easily be removed by a scale change).

The family of possible periodic solutions in the absence of free oscillations is labeled by the integer k,

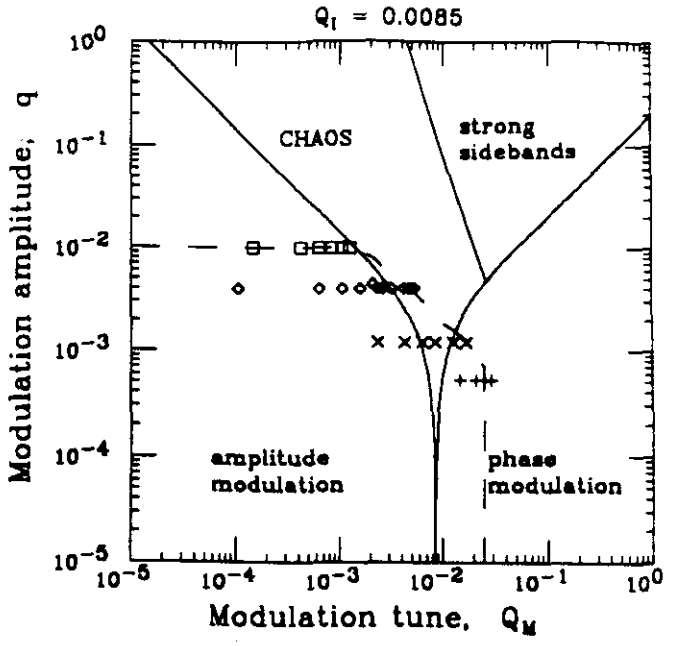

Figure 4. Dynamical behavior in different regions of the tune modulation parameter space (Q_M,q), for a value of Q_I = 0.0085. The dashed line shows the region accessible to the E778 experiment, extending beyond the resonance pole at $Q_M = Q_I$ for this particular value of the island tune. The symbols represent points at which data were taken (see Figure 5).

$$5\phi = k\, 2\pi (Q_M t) + \sum_{n=1}^{\infty} c_n \cos(n\, 2\pi Q_M t) \qquad [30]$$

by analogy with [8], where the coefficients c_n are functions of q, Q_M, and Q_I. The tune of the k-th solution is

$$Q_k = \frac{2}{5} + \frac{1}{2\pi} \left\langle \frac{d\phi}{dt} \right\rangle = \frac{2}{5} + k \frac{Q_M}{5} \qquad [31]$$

consistent with the set of sidebands predicted by [9]. Each sideband has five resonance islands, with centers at an action I_k given by $Q(I_k) = Q_k$, so

$$I_k = k \frac{2\pi Q_M}{5U} \ . \qquad [32]$$

These are the locations of *potential* sidebands—a given solution may or may not be stable, and may or may not have a significant strength. Rigorous analytical results for the solutions exist only in the slow and fast modulation limits, when Q_M is much smaller or much larger than Q_I. For large amplitude oscillations in the intermediate region it is necessary to rely on iterative solutions and on simulations.

The small angle k = 0 solution is illuminating. It is given, for all values of Q_M, by

$$\phi = \frac{Q_M^2}{Q_I^2 - Q_M^2} \frac{q}{Q_M} \cos(2\pi Q_M t)$$

and [33]

$$I = -\frac{Q_I^2}{Q_I^2 - Q_M^2} \frac{2\pi q}{U} \sin(2\pi Q_M t) \ .$$

Both expressions include the same resonance denominator, but with different numerators. At constant q, the amplitude of the action oscillation goes to $(2\pi q)/U$ for small Q_M and to zero for large Q_M, while the phase oscillation amplitude goes to zero for slow modulation, and to q/Q_M for fast modulation. This

explains the "amplitude modulation" and "phase modulation" labels in Figure 4. The small-angle approximation is only appropriate below the boundary line

$$\left|\frac{qQ_M}{Q_I^2 - Q_M^2}\right| = \frac{1}{5} \qquad [34]$$

which is the solid line in Figure 4 showing the "resonance" pole at $Q_M = Q_I$.

Rigorous analysis in the slow modulation limit (below) shows that when $Q_M << Q_I$ this solid line is also the boundary of stability for the $k = 0$ solution. Both simulations and a numerical iterative solution to [29] agree that just below the "resonance" condition, $Q_M \leq Q_I$, this line marks the limit of stability of the $k = 0$ fundamental, but that just above resonance the $k = 0$ solution is stable for all values of θ. This shows that the small angle boundary has different physical implications above and below the resonance. Preliminary results from the numerical iterative solution indicate that none of the $k \neq 0$ sideband solutions are stable below the resonance [5,7]. In contrast, all of the sideband solutions appear to be stable above resonance $Q_M \geq Q_I$, with the possible exception of a small region near the resonance.

Rigorous analysis in the large Q_M limit (also below) shows that, although the sidebands may be stable, the size of the islands is insignificant below the small angle boundary. If the sideband islands are big enough to overlap with each other and the fundamental chain of islands, there is large-scale chaos.

Slow modulation—the amplitude modulation region, $Q_M << Q_I$

If the tune is changing so slowly that the motion is adiabatic, it is reasonable to approximate the rate of change as constant. As will be seen, the most stringent conditions come when the rate of change is largest, so the most interesting approximation to the Hamiltonian in equation [27] is

$$H_5 = (2\pi)^2 qQ_M t\, I + \frac{1}{2} U I^2 - V\cos(5\phi) . \qquad [35]$$

This Hamiltonian is still time dependent, but now it is possible to go through a canonical coordinate transformation, from (I, ϕ, H_5) to $(\bar{I}, \bar{\phi}, \bar{H}_5)$, that produces a time independent Hamiltonian which can be graphically understood. Specifically [22], the generating function

$$F_3(I,\bar{\phi},t) = -I\bar{\phi} - \varepsilon t\bar{\phi} - \frac{1}{6}\varepsilon^2 t^3 \qquad [36]$$

with

$$\varepsilon = \frac{(2\pi)^2 qQ_M}{U} = 25\,V\frac{qQ_M}{Q_I^2} \qquad [37]$$

gives, by its definition,

$$\bar{I} = -\frac{\partial F_3}{\partial\bar{\phi}} = I + \varepsilon t\,, \quad \phi = -\frac{\partial F_3}{\partial I} = \bar{\phi} \qquad [38]$$

and

$$\bar{H}_5 = H_5 + \frac{\partial F_3}{\partial t} = \frac{1}{2}U\bar{I}^2 - V\cos(5\bar{\phi}) - \varepsilon\bar{\phi} . \qquad [39]$$

While the old phase and the new phase are identical, reflecting the suppression of phase modulation in this region, the new action drifts relative to the old action at a constant speed.

The new Hamiltonian has an extra term, linear in the phase, which has serious consequences for the stability of the $k = 0$ fundamental island chain. (Note that, as a consequence of linearizing the rate of change of tune, solutions with $k \neq 0$ are explicitly impossible in this picture). Pictorially, this non-periodic term corresponds to a constant slope of the quadratic valley of Hamiltonian contours, along the direction of the valley. If this slope is steep enough, there are no longer any local minima. There are minima, and the $k = 0$ solution exists, if there is a solution for the stable fixed point (I_{FP}, ϕ_{FP})

$$\begin{pmatrix} \frac{dI}{dt} \\ \frac{d\phi}{dt} \end{pmatrix} = \begin{pmatrix} -5V\sin(5\phi_{FP}) + \varepsilon \\ U I_{FP} \end{pmatrix} = \begin{pmatrix} 0 \\ 0 \end{pmatrix} \qquad [40]$$

where the overbars have been dropped. If the $k = 0$ islands exist, their centers are at $I_{FP} = 0$, with a shifted phase. There are no stable islands at all if $|\varepsilon| > 5V$, that is, if

$$\frac{qQ_M}{Q_I^2} > \frac{1}{5} . \qquad [41]$$

This condition corresponds, in the slow modulation limit, to the small angle boundary in equation [34].

Figure 5 shows the effect that entering the chaotic region has on the decay rate of persistent signals observed in the E778 experiment. A set of symbols of a particular kind represents a single constant value of q, at a series of Q_M values, corresponding to the data points plotted in Figure 4. A decay time of 47,000 turns is approximately equivalent to one second in the Tevatron. The decay rate increases dramatically when the stability boundary is crossed, consistent with a fit to the data of $Q_I = 0.0085$. Unfortunately, this method of measuring Q_I is time intensive, since each data point corresponds to a two-minute injection cycle of the Tevatron and the analysis is done off-line. It is hoped that in the near future it will be possible to measure Q_I in a single machine cycle, opening up the possibility of a rapid comprehensive scan of resonances across a relatively wide range of tunes.

Rapid modulation — the phase modulation region, $Q_M >> Q_I$

In this region, instead of approximating the old Hamiltonian and then applying a generating function, a time independent Hamiltonian is found by first applying a generating function and then making an approximation. The appropriate generating function is now

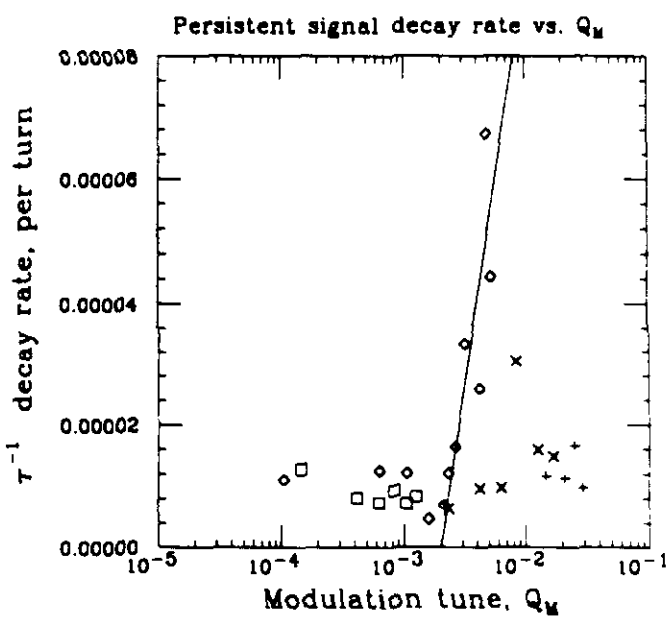

Figure 5. The effect of tune modulation on the decay rate of a persistent signal. Data taken at four values of q reaches from the amplitude modulation region just into the phase modulation region, and into the chaos region. The decay rate of the persistent signal increases significantly as the boundary between amplitude modulation and chaos is crossed.

$$F_3(I,\bar{\phi},t) \;=\; -I\bar{\phi} - \frac{q}{Q_M}\cos(2\pi Q_M t)\, I \qquad [42]$$

which gives, instead of [38] and [39],

$$\bar{I} = I,\ \phi = \bar{\phi} + \frac{q}{Q_M}\cos(2\pi Q_M t) \qquad [43]$$

and

$$\bar{H}_5 \;=\; \frac{1}{2}U\bar{I}^2 - V\cos(5\bar{\phi} + \frac{5q}{Q_M}\cos(2\pi Q_M t))$$

$$= \frac{1}{2}U\bar{I}^2 - V\sum_i J_i\,(\frac{5q}{Q_M})\cos(5\bar{\phi} + i\,2\pi Q_M t) \qquad [44]$$

where the J_i are integer order Bessel functions. In this transformation the action remains unchanged, but the phase is modified, appropriate to the phase modulation region. The Hamiltonian is made time independent by concentrating on the vicinity of the k-th sideband, near an action I_k, and then averaging the sum in [44] over one modulation period.

In the limit of large Q_M, not very much happens during one period, and only one turn in the sum survives the averaging. After resynchronising the Hamiltonian to concentrate on the k-th sideband, and dropping the overbars, then

$$H_{5k} \;=\; \frac{1}{2}\,U\,(I - I_k)^2 - V\,J_k\left(\frac{5q}{Q_M}\right)\cos(5\phi) \qquad [45]$$

which is time independent, and differs from the simple resonant form [19] mainly by the presence of the J_k factor. Whether or not the k-th sideband is significant depends on the value of this Bessel function. As a rule of thumb, J_k is approximately zero if the absolute value of the argument is less than the absolute value of k, the order. That is, the sideband k is only significant if

$$q > |k|\,\frac{Q_M}{5} \qquad [46]$$

The right hand side of this equation is the separation of the sideband tune from the fundamental resonance tune. Equation [46] therefore corresponds to the sensible physical condition that, in order for the resonance to be felt at actions near I_k, the tune of such trajectories must be modulated far enough to cross the fundamental.

The preceding argument implicitly assumes that the sidebands can be isolated one from the other, and treated separately. This is true if the sideband separation in action, $(2\pi Q_M)/5U$ according to [32], is larger than the sideband width. If the sidebands are typically wider than they are apart, chaos appears, spanning the action range of the sidebands of significant size [6, 8, 10, 23, 24]. It is easily shown by further approximating the Bessel function, and substituting $J_k V$ for V in [25], that sideband overlap is expected if [46] is true, and if

$$Q_M^{\,3/4}\,(5\,q)^{1/4} \;<\; \frac{4}{\pi^{1/4}}\,Q_I\ . \qquad [47]$$

This boundary is shown as the second solid line, nearly vertical, in Figure 4. Because of the "statistical" approximation of Bessel functions (similar in spirit to approximating a sin function by $1/\sqrt{2}$), this condition is rather qualitative. Depending on the exact phase of the sidebands, some will overlap earlier or later than the condition suggests.

A Beam-Beam Example of Sideband Overlap

Figure 6 shows the appearance of sideband islands when tune modulation with $Q_M > Q_I$ is turned on, in the presence of a single beam-beam interaction with a tune shift parameter just below and just above the critical value required for sideband overlap [21]. The success of equation [47] in predicting this overlap can be seen as follows. Substituting the values Q_M = 0.0052 and q = 0.001, and replacing the resonance order 5 with 6, then the equation predicts that if Q_I is greater than 0.0018, chaos ensues. Since the amplitude of the fundamental resonance is held constant at 2.7 σ in the simulation, then according to Figure 2 the value of Q_I/ξ is about 0.37, leading to a prediction of about 0.0048 for the critical value of the tune shift parameter. This is in surprisingly good agreement with the simulation, considering the approximations which entered into the derivation of [47].

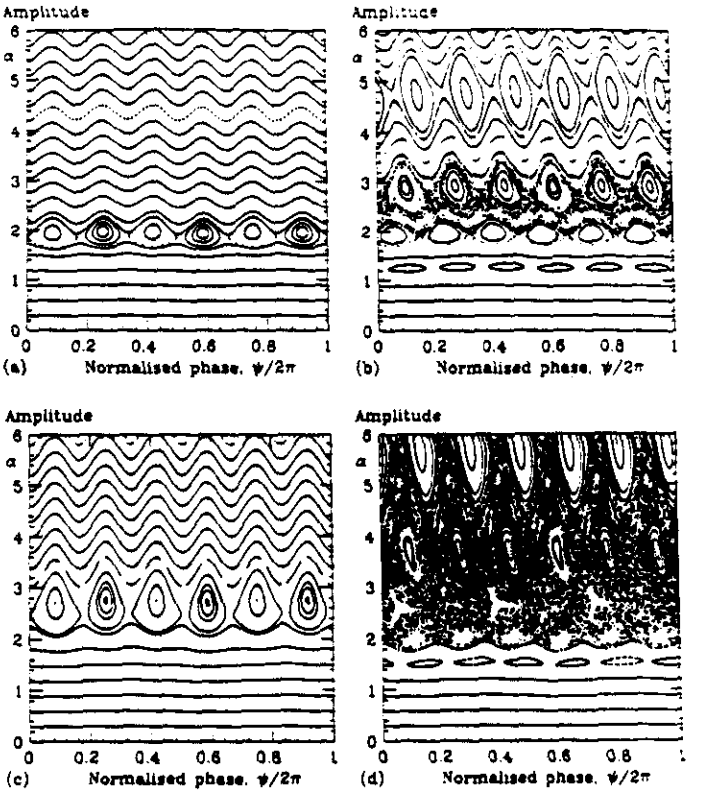

Figure 6. The creation of resonance sidebands, and their chaotic overlap, by tune modulation. A single round beam-beam interaction of strength ξ perturbs the phase space, with a base tune near a sixth order resonance. Plots a) and b), on top, have ξ = 0.0042, while the bottom two plots have a slightly stronger value ξ = 0.006 . Plots a) and c), on the left, have no tune modulation, while those on the right have (Q_M,q) = (1/194, 0.001). Sidebands become visible when the modulation is turned on in b), but the sidebands must overlap for massive chaos to occur, in d). Amplitude α is measured in units of the beam size.

ACKNOWLEDGEMENTS

Thanks are due to many members of the E778 collaboration, and others, for the direct and indirect contributions that they have made to this paper. Miguel Furman first pointed out the connection between driven pendula and Josephson junctions, and helped improve the prose of this paper. Richard Kautz has been a mine of information about driven Josephson junctions. Last, but not least, Annie Calinog and Valerie Kelly made it possible to produce this paper on a very tight schedule. Our thanks to you all.

REFERENCES AND FOOTNOTES

1. A. Piwinski, *IEEE Trans. Nucl. Sci.*, vol. 24: 3, 1977.
2. S. Peggs, and R. Talman, *Phys. Rev. D*, vol. 24, p.2379, 1981.
3. S. Myers, LEP Note 362, CERN, Geneva, 1982.
4. J. Seeman, SLAC-PUB-3182, Stanford, 1983.
5. E. Keil and R. Talman, *Particle Accelerators*, vol. 14, pp. 109–118, 1983.
6. E. Courant, ISABELLE Technical Note No. 163, Brookhaven, 1980.
7. F. M. Izrailev, S. I. Misnev and G. M. Tumaikin, Preprint 77–43, Novosibirsk, 1977.
8. J. Tennyson, *AIP Conf. Proc.* 57, New York, 1979.
9. L. Evans and J. Gareyte, *IEEE Trans. Nucl. Sci.* vol 30: 4, 1982.
10. S. Peggs, *Particle Accelerators*, vol. 17, pp.11–50, 1985.
11. D. B. Sullivan and J. E. Zimmerman, *AJP*, vol. 39, p.1504, 1971.
12. C. K. Bak and M. P. Pedersen, *Applied Physics Letters*, vol. 22:4, 1973.
13. Rochlin and Hansma, *AJP* vol. 41, p. 878, 1973.
14. R. Kautz, private communication, 1989.
15. N. Merminga, "A study of nonlinear dynamics in the Fermilab Tevatron," PhD. Thesis, University of Michigan, 1989.
16. D. Edwards and M. Syphers, "An overview of experiment E778," *Proc. of the ICFA Workshop, Lugano*, 1988.
17. A. Chao, et al., "Experimental investigation of nonlinear dynamics in the Fermilab Tevatron," *Physical Review Letters*, vol. 61, p. 2752, December 12, 1988.
18. T. Chen and S. Peggs, "Tune modulation and the driven differential pendulum, " to be published in *Proc. of the IEEE Particle Accelerator Conference, Chicago*, 1989.
19. S. Peggs, C. Saltmarsh, and R. Talman, "Million revolution accelerator beam instrument for logging and evaluation," SSC-169, Berkeley, 1988.
20. S. Peggs, "Hamiltonian theory of the E778 nonlinear dynamics experiment," SSC-175, Berkeley, 1988.
21. S. Peggs and R. Talman, "Nonlinear problems in accelerator physics," *Annual Reviews of Nuclear Science*, vol. 36, pp. 287–325, 1986.
22. H. Goldstein, *Classical Mechanics*. Addison-Wesley, Menlo Park, 1980.
23. B. Chirikov, *Phys. Rep.* vol. 20, p.265, 1979.
24. A. Lichtenberg and M. Lieberman, *Regular and Stochastic Motion*. Springer-Verlag, New York, 1983.